ARTICLES
PUBLISHED ONLINE: 26 JANUARY 2015 | DOI: 10.1038/NCHEM.2161
nature chemistry

Coulomb explosion during the early stages of the reaction of alkali metals with water

Philip E. Mason[1], Frank Uhlig[1], Václav Vaněk[1], Tillmann Buttersack[2], Sigurd Bauerecker[2] and Pavel Jungwirth[1]*

Alkali metals can react explosively with water and it is textbook knowledge that this vigorous behaviour results from heat release, steam formation and ignition of the hydrogen gas that is produced. Here we suggest that the initial process enabling the alkali metal explosion in water is, however, of a completely different nature. High-speed camera imaging of liquid drops of a sodium/potassium alloy in water reveals submillisecond formation of metal spikes that protrude from the surface of the drop. Molecular dynamics simulations demonstrate that on immersion in water there is an almost immediate release of electrons from the metal surface. The system thus quickly reaches the Rayleigh instability limit, which leads to a 'coulomb explosion' of the alkali metal drop. Consequently, a new metal surface in contact with water is formed, which explains why the reaction does not become self-quenched by its products, but can rather lead to explosive behaviour.

Throwing a piece of sodium or potassium into water is an all-time favourite classroom demonstration of a vigorous chemical process[1]. For the very same reasons, contact with water needs to be strictly avoided when liquid sodium or sodium/potassium alloys are used as the primary coolant in fast neutron nuclear reactors, whereas a controlled reaction with water can be employed in subsequent decommissioning of the used alkali metal[2]. Mechanistically, dissolving alkali metals in water is a strongly exothermic process in which electrons move from the metal into the aqueous solution where they react to form hydroxide and hydrogen. The related heat release can be sufficient for melting of the metal, massive steam formation and ignition of the hydrogen gas, which leads to an explosive behaviour[3]. If the produced hydrogen is ignited then the sodium reaction with water produces more energy than the explosion of an equivalent mass of trinitrotoluene[4]. However, for a heterogeneous process in which the reaction can only occur at the interface, an efficient mixing of the reactants needs to be ensured for it to become explosive[5]. It is not clear how such a mixing between the macroscopically heterogeneous alkali metal and water is achieved. Indeed, production of steam and hydrogen gas at the contact between water and metal should lead to the formation of a vapour layer that physically separates the reactants[6] and thus inhibits further reaction. Here we present the results of high-speed camera imaging complemented by molecular dynamics simulations and reveal that a 'coulomb explosion', which is characterized, in this case, by metal spikes protruding into water, plays an important role in triggering subsequent explosive behaviour. The coulomb explosion is caused by a massive charging of the surface of the liquid metal with the fast migration of electrons into water, which precedes and actually enables the notoriously explosive alkali metal–water reaction.

Results

High-speed camera imaging. The problem with systematically investigating explosions of alkali metals in water is that the process is erratic; it sometimes leads to an explosive behaviour and sometimes not. The outcome depends on many factors, such as the choice of the particular alkali metal, cleanliness of its surface, velocity with which the metal hits the water, temperature and so on[2,7]. After much experimentation we devised a strategy that allows us to investigate the explosive behaviour of alkali metals in water in a reproducible way. The two key ingredients of our set-up are as follows (for details, see Methods and Supplementary Section 3). First, we employ a Na/K alloy (~90 wt% K) that is liquid at room temperature[8]. Under an argon atmosphere this allows us to use a syringe to drop a well-defined amount of the metal alloy (~100 mg) with an always fresh (unoxidized) surface from a given height (typically 1 m) into water, which leads to fully reproducible explosions. Second, we use high-speed cameras to follow the process with a ~100 μs time resolution. Such a time resolution is crucial to capture the early stage of the explosive process, which turns out to hold the key to an explanation of its mechanism in a rather unexpected way (*vide infra*).

Figure 1 presents a series of snapshots from a high-speed camera of a Na/K drop hitting water compared (as a control) with an analogous process for a water drop, which has a roughly equivalent density and surface tension (for the corresponding video see Supplementary Movie 1). A vigorous reaction starts within a fraction of a millisecond of the Na/K drop impacting on the water, compared to the purely hydrodynamic effects observed for the water drop. The metal drop of diameter about 6 mm touches the water surface and after 0.5 ms the explosion is in full process with extensive gas production. The crucial snapshot is, however, the one at $t = 0.35$ ms (that is, the fifth snapshot from the top in the middle column of Fig. 1). Here we can clearly see metal spikes that protrude into the water from the Na/K drop and that shoot out of the surface of the drop with an acceleration of the order of 10,000 m s^{-2} (estimated using the fact that the onset of spike formation is already visible in the previous snapshot at $t = 0.26$ ms). Closer inspection of the filmed time frames reveals that the process of spike formation can be of a dendritic nature, in which new spikes shoot out from already formed ones. The formation of metal spikes is evidently happening faster than the production of gas (Fig. 1). Also, the submillisecond timescale of the spike formation rules out the possibility that this could be a thermally driven process at the surface of a hot

[1]Institute of Organic Chemistry and Biochemistry, Academy of Sciences of the Czech Republic, Flemingovo nám. 2, 16610 Prague 6, Czech Republic.
[2]Institut für Physikalische und Theoretische Chemie, Technische Universität Braunschweig, Hans-Sommer-Strasse 10, D-38106 Braunschweig, Germany.
*e-mail: pavel.jungwirth@uochb.cas.cz

© 2015 Macmillan Publishers Limited. All rights reserved

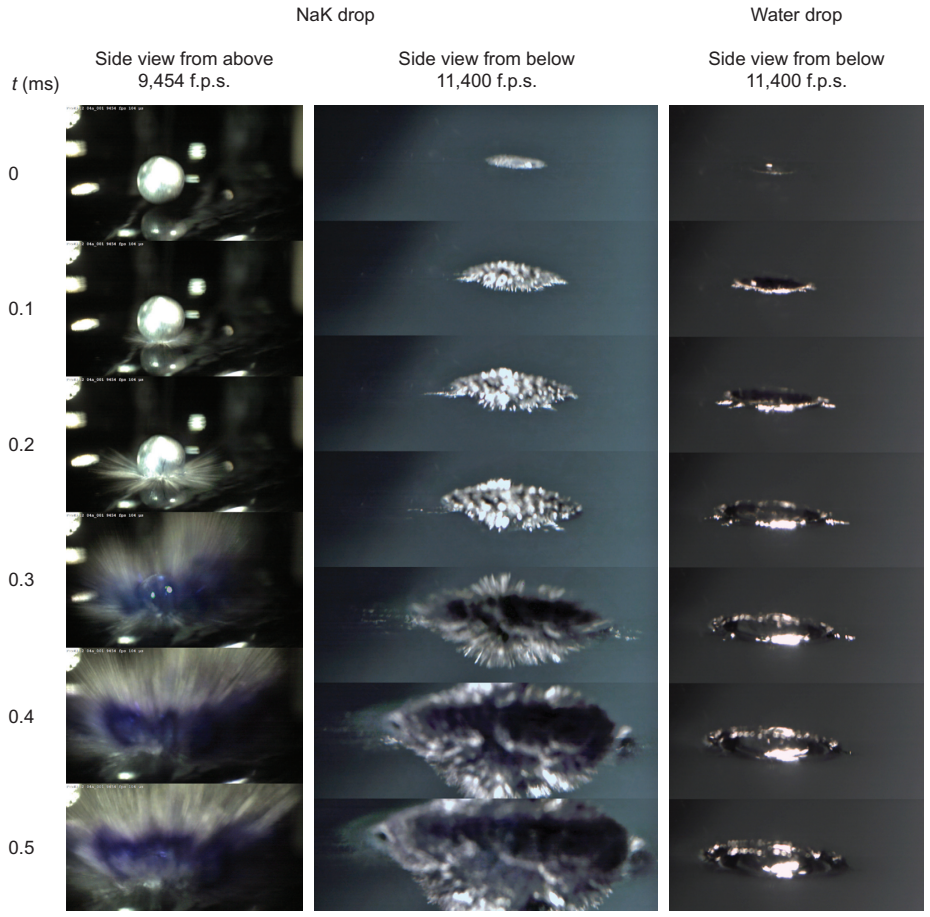

Figure 1 | High-speed camera images of a Na/K alloy drop versus a water drop impacting on water. The left and middle columns feature side views of the Na/K alloy drop from above and below the surface from two separate experiments. The right column is the side view of a water drop from below the surface, shown for comparison. For the alloy drop the metal spikes clearly protrude from the surface (best seen in the middle column at 0.3–0.4 ms) before subsequent explosion, whereas for the water drop only hydrodynamic effects are present. The blue colour in the last three frames in the left and middle columns is caused by the absorption of solvated electrons. The filming rates were 9,454 or 10,400 f.p.s. with an illumination time for each frame of 49 μs. For the corresponding videos see Supplementary Movie 1.

metal[9]. In a test experiment we put a drop of a similar size of molten aluminium (at ~1,000 °C) in water and no comparable spike formation was observed. Instead, a Leidenfrost effect[6] occurred in which steam kept the two liquids separate on a 100 ms timescale.

The phenomenon of alkali-metal-spike formation in water is of a transient nature and in less than a millisecond becomes completely overwhelmed by the subsequent gas production. Although the spikes appear to be the direct source of the rapid increase in reactive surface area, it is the production of gas that causes the explosion. That the formation of spikes does not require an explosion to take place can be demonstrated by repeating the experiment in liquid ammonia (at −77.8 °C) instead of water. Again, transient spikes are formed (Fig. 2), albeit less clearly than in water. Also, unlike in water, the reaction of the alkali metal with liquid ammonia does not produce hydrogen rapidly and no explosion happens.

The dark blue/black regions in Fig. 2 result from light absorption by electrons solvated in ammonia[10]. In liquid ammonia, solvated electrons are long-lived and thus easily observable (which is well-known to organic chemists who perform the Birch reduction), whereas in water their lifetime is shorter than a millisecond[11]. As a result, as yet they have not been observed in water directly by the naked eye; nevertheless, the blue colour in the last three snapshots in Fig. 1 (left and middle columns) represents a fingerprint of these transient hydrated electrons. Knowing that the extinction coefficient of solvated electrons[12] is 18,400 m^{-1} M^{-1} and qualitatively estimating from the snapshots a two orders of magnitude drop in light intensity over a ~1 cm thick layer of blue colour, we obtain a concentration of the solvated electrons of about 0.1 mM. Incidentally, this electron concentration is comparable to that obtained in ultrafast photoionization experiments in aqueous solutions[13].

***Ab initio* molecular dynamics.** What could be the force that shoots spikes from the alkali metal surface into water with such a large acceleration? To shed more light on the molecular mechanism of this process we performed *ab initio* molecular dynamics (AIMD) simulations of a microscopic model of the experimental system, namely, a medium-sized cluster of 19 sodium atoms immersed in water (for details, see Methods and Supplementary Section 1). The dynamics occurs on the ground-state surface, which is clearly an approximation, but this is supported by recent ultrafast experiments[14]. These experiments show that non-equilibrium electrons in water relax fast electronically, after which the dynamics proceeds in the ground electronic state. Figure 3 demonstrates how the cluster expands in water and the 17 surface sodium atoms each lose an electron quickly, within several picoseconds (for the corresponding video see Supplementary Movie 2). These electrons dissolve in water and react in pairs to form molecular hydrogen and hydroxide in a process that has previously been modelled in detail for smaller systems[15,16]. Most importantly for the phenomenon investigated here, the surface of the sodium cluster thus acquires a large positive charge almost immediately after coming into contact with water (Fig. 3).

© 2015 Macmillan Publishers Limited. All rights reserved

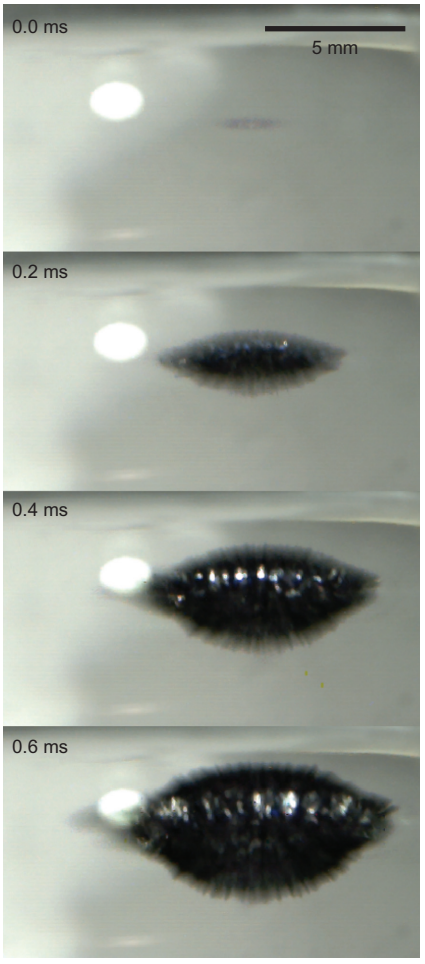

Figure 2 | High-speed camera images of a Na/K alloy drop impacting on liquid ammonia. In a side view from below the surface, metal spikes can be seen to form at the surface of the drop. The dark blue/black colour results from the absorption of the solvated electrons. The frame rate was 5,000 f.p.s. with an illumination time for each frame of 197 μs.

Force-field molecular dynamics. Based on the above observation from AIMD of a rapid charging of the cluster surface, we set up force-field molecular dynamics (FFMD) simulations of much larger clusters that are computationally inaccessible by AIMD. The present system contains 4,000 sodium atoms, which on contact with water become positively charged and the negative charge moves into the aqueous phase (for details see Methods and Supplementary Section 1). Such a system is still significantly smaller than the experimental one; nevertheless, the modelled piece of metal already has well-developed surface and interior regions. In the simulations, the sodium cluster is immersed in water and surrounded by hydroxide anions that compensate its positive charge. For a larger-than-critical separation of the positive and negative charges of about 5 Å (Fig. 4 and *vide infra*) the coulomb repulsion at the sodium surface leads to a rapid expansion and disintegration of the cluster in the aqueous solution. The simulated system is too small to reproduce faithfully the formation of the macroscopic metal spikes observed in the experiment, but nevertheless the partial disintegration of the sodium cluster in a spike-like manner that results from the surface coulomb repulsion is clearly visible in Fig. 4 (for the corresponding video, see Supplementary Movie 3).

Discussion

The above experimental and computational observations are reminiscent of a related process of coulomb fission or coulomb explosion,

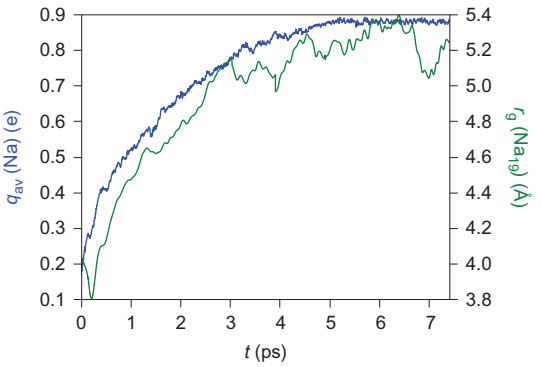

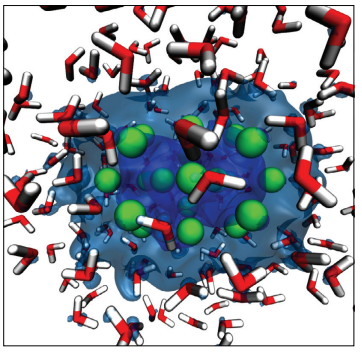

0 ps

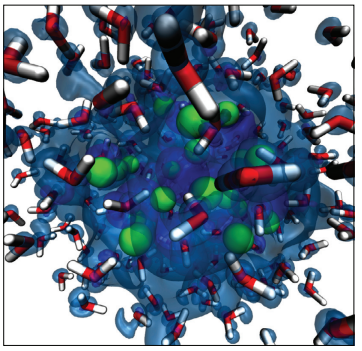

1 ps

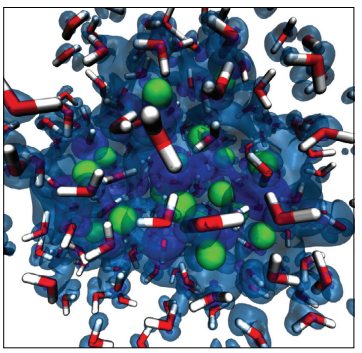

2 ps

Figure 3 | AIMD simulations of the time evolution of the radius of gyration (green) and the average charge on a sodium atom (blue) of a medium-sized sodium cluster in water. Within a few picoseconds all the surface sodium atoms lose an electron. These electrons move to the water, where they react to form molecular hydrogen and hydroxide. At the same time the cluster expands. The individual snapshots show the sodium atoms (green balls), water molecules (red–white sticks) and the electrons dissolving in water (blue differential electron-density contours) along the trajectory (Supplementary Movie 2).

© 2015 Macmillan Publishers Limited. All rights reserved

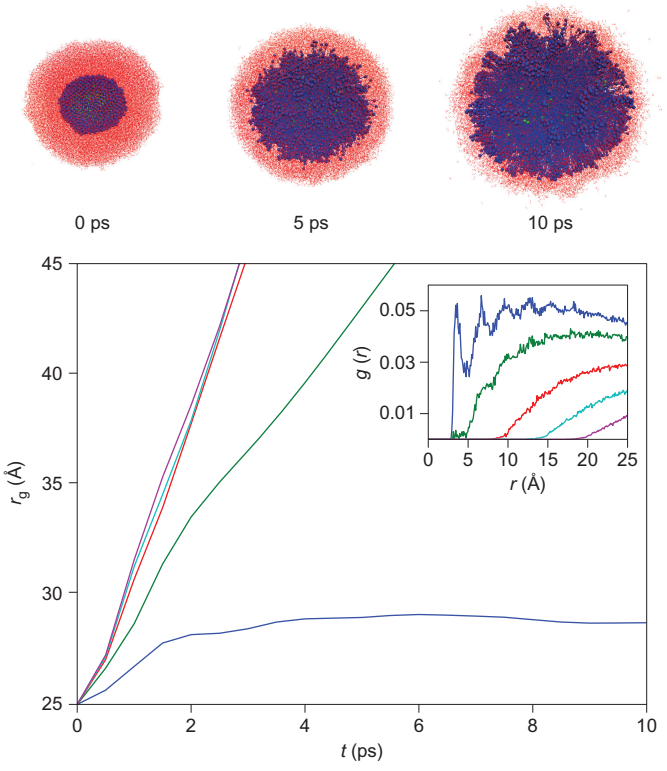

Figure 4 | Time evolution of the radius of gyration of a large sodium cluster surrounded by water for different values of the initial separation of the positive and negative charges. The inset shows the corresponding initial radial distributions of the negatively charged hydroxide ions with respect to all sodium atoms. There is a fast increase of the size and disintegration of the cluster in a spike-like fashion for charge separations above a critical value of about 5 Å. In snapshots that correspond to this critical value the neutral sodium atoms are depicted as green balls, sodium ions as blue balls, and water and hydroxides are in red (also see Supplementary Movie 3).

well-known from gas-phase studies, that has been shown to be the mechanism behind the breakup of charged droplets in electrospray or following multiple ionization[17–20]. It has been demonstrated that, on charging, droplets in the gas phase can reach the Rayleigh instability limit[19,21]. Consequently, these droplets undergo coulomb fission by shooting out one or two spikes (so-called Taylor cones or Rayleigh jets), or even multiples of them, within a coulomb explosion process if the charging is more extensive[17–20]. However, in bulk water the counter-charges are present in the liquid next to the charged drop and, to our knowledge, such a mechanism has not been invoked yet. The key question in this respect is whether the Rayleigh instability limit[19,21] for the Na/K drop in water can be overcome, as is the case for the gas-phase droplets in electrospray or in intense ionizing laser fields. This limit for coulomb fission is reached when the fissility parameter X, defined as the ratio between the droplet coulomb self-energy and twice its surface energy ($X = E_{coulomb}/2E_{surface}$), exceeds unity[19]. Knowing the surface tension of the Na/K drop[8,22] and assuming that by moving electrons from its surface atoms to water, an effective capacitor is formed with a mean charge separation (d), one can estimate that the drop becomes coulombically unstable for $d > 5$ Å (for a detailed derivation see Supplementary Section 2). This very small distance corresponds to slightly more than a single water layer and our AIMD simulations show that the electrons or the subsequently formed hydroxide anions reach such a mean separation from the surface of a Na/K drop on a picosecond timescale. The above force-field simulations also demonstrate that this back-of-the-envelope estimate of the critical charge separation of about 5 Å is remarkably accurate (Fig. 4).

Thus, the above molecular simulations and estimates concerning the Rayleigh instability limit strongly support the notion that the metal spikes observed by high-speed cameras in the early stages of dissolution of a Na/K drop result from electrostatic repulsion of the alkali cations formed at its surface by an almost immediate release of electrons into water, which leads to a coulomb explosion. As a matter of fact, without invoking the coulomb-explosion mechanism, the alkali/water interface should become passivated by the steam and hydrogen gas formed, as well as the hydroxide; consequently, no explosion could occur. This conclusion is further supported by the fact that we were able to kill the explosion completely by adding small amounts of a surface-active species, such as hexanol, to water before dropping the alkali metal alloy into it. Impurities at both the water and alkali metal surfaces are among the reasons why the classroom-type demonstrations of the vigorous sodium reaction in water may or may not lead to explosions in a rather erratic way. Nevertheless, when a piece of sodium does explode in water it first melts into a liquid drop because of the heat release and low melting point[3], after which the explosive behaviour is analogous to that of the Na/K drop investigated in a controlled way in the present study.

In conclusion, based on direct experiments using high-speed cameras and molecular simulations, we suggest that the early stage of the vigorous dissolution of a Na/K alloy drop in water is driven by a coulomb explosion. This process is initiated by electrostatic repulsion within a layer of alkali cations formed at the surface of the drop and caused by an almost immediate release of the alkali metal valence electrons into water. The resulting Rayleigh instability leads to the formation of metal spikes that shoot into the water. This process, in turn, produces a new surface at which the heterogeneous alkali metal–water reaction can propagate further in an explosive way.

Methods

Experimental. A Na/K alloy (~90 wt% K) was prepared by cutting 5.0 g potassium (98% Sigma Aldrich) and 0.5 g sodium (99.9%, Sigma Aldrich) into small pieces and squeezing the two metals together under pentane in a Nalgene vial. To remove the bulk of any oxide formed the alloy was then transferred using a polypropylene syringe to a new vial that contained pentane. Finally, one drop of isopropyl alcohol was added. This yielded a 'mirror shiny' ball of a Na/K alloy.

For the explosion experiments, an argon supply was attached to one arm of a three-necked Quickfit flask. A 1 m long glass tube was fitted to the central arm and 20 ml of pure water was added through the third arm. Once the apparatus had been flushed with argon, a single drop of the Na/K alloy was dropped from the top of the 1 m tubing. The size of the drop was determined by the surface tension of the metal and its adhesion to the 1 ml polypropylene syringe. This resulted in a reproducible drop weight of 80–100 mg. When the Na/K alloy impacted on the surface, an explosion was observed in more than 99% of cases. However, when water was replaced by a 0.5 wt% aqueous solution of hexanol, the Na/K alloy did not explode on impact, but fizzed around on the surface. We also probed other surface-active impurities with a similar result.

The experiment in liquid ammonia was set up in an analogous manner. Prior to the experiment, the joints of the three-necked flask were covered with a high-vacuum silicone grease to avoid humidity infiltration. The apparatus was flushed with dry argon, and the flask was then immersed in a liquid-nitrogen bath fed with a stream of pure gaseous ammonia. After about 20 ml of partially solidified ammonia had been collected, the cooling bath was removed and the flask was flushed continuously with a stream of argon to minimize the contact of the alloy drop with ammonia vapour. After all the solidified ammonia had melted (at −77.8 °C), the Na/K alloy drop was introduced as in the experiment in water. A temperature-regulated nitrogen cold-gas flow from a gas-cycle refrigeration system from KGW was used to adjust precisely the temperatures from the ammonia melting point up to −34 °C.

The experiments were monitored using three high-speed cameras from Imaging Solutions (IDT Motion ProY4 black-and-white 5,100 frames per second (f.p.s.) @1,016 × 1,016 pixel, IDT MotionXtra NR4 colour 3,000 f.p.s.@1,024 × 1,024 pixel and IDT Motion ProY3 colour 6,000 f.p.s.@1,280 × 1,024) using recording rates up to 37,000 f.p.s. in combination with different macro objectives (mostly Nikon 105 mm). Various camera angles were used in the standard arrangement with two simultaneously recording cameras, one from the bottom side and the other from the top side of the water surface. The needed illumination power was delivered by two KLQ350 xenon electric-arc sources from Henning Faseroptik via four fibre-optic light guides, including concentration lenses.

© 2015 Macmillan Publishers Limited. All rights reserved

Needless to say, strict safety precautions must be taken when performing these potentially dangerous experiments, as described in more detail in Supplementary Section 3.

Computational. Both AIMD and FFMD were carried out for sodium in water. Structures for the AIMD were prepared from isolated sodium clusters of 19 atoms, and were optimized first using a force field and then using density functional theory methods, which were also used later in the simulations. The clusters were then solvated by up to 174 water molecules and the water structure was relaxed, but with argon atoms at the positions of the sodium atoms to avoid a premature initiation of the reaction. The positions of the argon atoms were kept fixed during the minimization. The resulting snapshots were then used as starting structures for the production runs at constant energy and volume, with velocities initialized according to a Maxwell–Boltzmann distribution at 300 K. The charge on the sodium cluster was established using Bader's atoms-in-molecules analysis[23].

The AIMD simulation set-up was as follows. The wavefunction was expanded into an atom-centred triple-zeta basis set with polarization functions and an auxiliary basis set of plane waves with a cutoff of at least 400 Ry (ref. 24). Norm-conserving, relativistic pseudopotentials of a Goedecker–Teter–Hutter type replaced the core 1*s* electrons[25]. Newton's equations of motion were integrated with the velocity Verlet propagator and a time step of 0.5 fs. Forces were obtained from the combined Becke exchange and the Lee–Yang–Parr correlation functional[26,27]. An additional, pairwise-additive term that effectively accounted for the dispersion interactions was included[28]. Poisson's equation for the isolated systems was solved using a wavelet-based algorithm and in a cell size of 35 Å (ref. 29). The CP2K program was employed for the AIMD simulations[30].

Consequently, the initial structures were prepared for extended FFMD simulations in which a cluster that consisted of 4,000 sodium atoms was surrounded by 34,717 water molecules. Sodium atoms were alchemically changed into sodium cations within about two picoseconds on contact with at least three water molecules and, for charge compensation, hydroxide ions were created in a spherical shell around the sodium atoms in the aqueous phase. The OPLS/AA force field was used for sodium cations and hydroxide anions[31], whereas a specially developed force field was employed for neutral sodium atoms[32]. An extended simple point-charge model was used for water[33]. The force fields for ions and water are standard ones that have been shown to provide a reliable description of the corresponding aqueous systems[34,35], particularly for the very robust observables (such as the time evolution of the mean cluster size) we follow in the present study. The only non-standard feature is the gradual transmutation of sodium atoms into sodium cations on contact with water, which was parameterized based on the above AIMD simulations. A large cutoff of 5 nm was used for both coulomb and van der Waals interactions. The program suite GROMACS was used for FFMD simulations[36].

Received 7 October 2014; accepted 12 December 2014; published online 26 January 2015

References

1. Hutton, A. T. Dramatic demonstration for a large audience – the formation of hydroxyl ions in the reaction of sodium with water. *J. Chem. Educ.* **58,** 506 (1981).
2. Carnevali, S., Proust, C. & Soucille, M. Unsteady aspects of sodium–water–air reaction. *Chem. Eng. Res. Design* **91,** 633–639 (2013).
3. Krebs, R. E. *The History and Use of Our Earth's Chemical Elements* (Greenwood Press, 2006).
4. Commander, J. C. An explosive hazard analysis of the eutectic solution of NaK and KO_2. *Nucl. Sci. Abstracts* **32,** 21922 (1975).
5. Mukasyan, A. S., Khina, B. B., Reeves, R. V. & Son, S. F. Mechanical activation and gasless explosion: nanostructural aspects. *Chem. Eng. J.* **174,** 677–686 (2011).
6. Bernardin, J. D. & Mudawar, I. A cavity activation and bubble growth model of the Leidenfrost point. *J. Heat Transfer* **124,** 864–874 (2002).
7. Grubelnik, A., Meyer, V. R., Buetzer, P. & Schoenenberger, U. W. Potassium metal is explosive – do not use it! *J. Chem. Educ.* **85,** 634 (2008).
8. Alchagirov, B. B. *et al.* Surface tension and adsorption of components in the sodium–potassium alloy systems: effective liquid metal coolants promising in nuclear and space power engineering. *Inorg. Mater. Appl. Res.* **2,** 461–467 (2011).
9. Buchanan, D. J. & Dullforc, T. A. Mechanism for vapor explosions. *Nature* **245,** 32–34 (1973).
10. Gibson, G. E. & Argo, W. L. The absorption spectra of the blue solutions of certain alkali and alkaline earth metals in liquid ammonia and in methylamine. *J. Am. Chem. Soc.* **40,** 1327–1361 (1918).
11. Hart, E. J. Research potentials of hydrated electron. *Acc. Chem. Res.* **2,** 161–167 (1969).
12. Christensen, H. & Sehested, K. The hydrated electron and its reactions at high temperatures. *J. Phys. Chem.* **90,** 186–190 (1986).
13. Vilchiz, V. H., Kloepfer, J. A., Germaine, A. C., Lenchenkov, V. A. & Bradforth, S. E. Map for the relaxation dynamics of hot photoelectrons injected into liquid water via anion threshold photodetachment and above threshold solvent ionization. *J. Phys. Chem. A* **105,** 1711–1723 (2001).
14. Elkins, M. H., Williams, H. L., Shreve, A. T. & Neumark, D. M. Relaxation mechanism of the hydrated electron. *Science* **342,** 1496–1499 (2013).
15. Mundy, C. J., Hutter, J. & Parrinello, M. Microsolvation and chemical reactivity of sodium and water clusters. *J. Am. Chem. Soc.* **122,** 4837–4838 (2000).
16. Mercuri, F., Mundy, C. J. & Parrinello, M. Formation of a reactive intermediate in molecular beam chemistry of sodium and water. *J. Phys. Chem. A* **105,** 8423–8427 (2001).
17. de la Mora, J. F. On the outcome of the coulombic fission of a charged isolated drop. *J. Colloid Interface Sci.* **178,** 209–218 (1996).
18. Duft, D., Achtzehn, T., Muller, R., Huber, B. A. & Leisner, T. Coulomb fission – Rayleigh jets from levitated microdroplets. *Nature* **421,** 128–128 (2003).
19. Echt, O., Scheier, P. & Mark, T. D. Multiply charged clusters. *C. R. Phys.* **3,** 353–364 (2002).
20. Last, I., Levy, Y. & Jortner, J. Beyond the Rayleigh instability limit for multicharged finite systems: from fission to coulomb explosion. *Proc. Natl Acad. Sci. USA* **99,** 9107–9112 (2002).
21. Rayleigh, L. On the equilibrium of liquid conducting masses charged with electricity. *Phil. Mag.* **14,** 184–186 (1882).
22. Lebedev, R. V. Measurements of interphase surface-tension of sodium–potassium alloys. *Izv. Vus. Fiz.* **15,** 155–158 (1972).
23. Yu, M. & Trinkle, D. R. Accurate and efficient algorithm for Bader charge integration. *J. Chem. Phys.* **134,** 064111 (2011).
24. VandeVondele, J. & Hutter, J. Gaussian basis sets for accurate calculations on molecular systems in gas and condensed phases. *J. Chem. Phys.* **127,** 114105 (2007).
25. Goedecker, S., Teter, M. & Hutter, J. Separable dual-space Gaussian pseudopotentials. *Phys. Rev. B* **54,** 1703–1710 (1996).
26. Becke, A. D. Density-functional exchange-energy approximation with correct asymptotic-behavior. *Phys. Rev. A* **38,** 3098–3100 (1988).
27. Lee, C. T., Yang, W. T. & Parr, R. G. Development of the Colle–Salvetti correlation-energy formula into a functional of the electron-density. *Phys. Rev. B* **37,** 785–789 (1988).
28. Grimme, S., Antony, J., Ehrlich, S. & Krieg, H. A consistent and accurate *ab initio* parametrization of density functional dispersion correction (DFT-D) for the 94 elements H–Pu. *J. Chem. Phys.* **132,** 154104 (2010).
29. Genovese, L., Deutsch, T., Neelov, A., Goedecker, S. & Beylkin, G. Efficient solution of Poisson's equation with free boundary conditions. *J. Chem. Phys.* **125,** 074105 (2006).
30. VandeVondele, J. *et al.* QUICKSTEP Fast and accurate density functional calculations using a mixed Gaussian and plane waves approach. *Comp. Phys. Commun.* **167,** 103–128 (2005).
31. Jorgensen, W. L. *OPLS and OPLS-AA Parameters for Organic Molecules, Ions, and Nucleic Acids* (Yale Univ. 1997).
32. Bhansali, A. P., Bayazitoglu, Y. & Maruyama, S. Molecular dynamics simulation of an evaporating sodium droplet. *Int. J. Thermal Sci.* **38,** 66–74 (1999).
33. Berendsen, H. J. C., Grigera, J. R. & Straatsma, T. P. The missing term in effective pair potentials. *J. Phys. Chem.* **91,** 6269–6271 (1987).
34. Kastenholtz, M. A. & Hunenberger, P. H. Computation of methodology-independent solvation free energies from molecular simulations. II. The hydration free energy of the sodium cation. *J. Chem. Phys.* **124,** 224501 (2006).
35. Krizek, T. *et al.* Electrophoretic mobilities of neutral analytes and electroosmotic flow markers in aqueous solutions of Hofmeister salts. *Electrophoresis* **35,** 617–624 (2014).
36. Hess, B., Kutzner, C., van der Spoel, D. & Lindahl, E. GROMACS 4: algorithms for highly efficient, load-balanced, and scalable molecular simulation. *J. Chem. Theor. Comput.* **4,** 435–447 (2008).

Acknowledgements

We thank J. Jiráček for boldly making his chemical laboratory available to us for the initial experiments in liquid ammonia. P.J. acknowledges the Czech Science Foundation (Grant P208/12/G016) for support and thanks the Academy of Sciences for the Praemium Academiae award. S.B. acknowledges support from the Deutsche Forschungsgemeinschaft (Grants BA 2176/3–2 and BA 2176/4–1). P.E.M. acknowledges support from the viewers of his YouTube popular science channel.

Author contributions

P.E.M., S.B. and P.J. designed and analysed the experiments. P.E.M., V.V., T.B. and S.B. performed the experiments. F.U. and P.J. designed and analysed the simulations and F.U. executed the calculations. P.J. wrote the paper with critical feedback from all the co-authors.

Additional information

Supplementary information is available in the online version of the paper. Reprints and permissions information is available online at www.nature.com/reprints. Correspondence and requests for materials should be addressed to P.J.

Competing financial interests

The authors declare no competing financial interests.

© 2015 Macmillan Publishers Limited. All rights reserved